Pilot-added carrier-phase recovery scheme for Nyquist M-ary quadrature amplitude modulation optical fiber communication system

Wenbo Zhang (张文博)[1,*], Dongwei Pan (潘董威)[2], Xiaofei Su (宿晓飞)[2], Xiaoguang Zhang (张晓光)[2,], Lixia Xi (席丽霞)[2], and Xianfeng Tang (唐先锋)[2]**

[1]*School of Science, Beijing University of Posts and Telecommunications, Beijing 100876, China*
[2]*State Key Laboratory of Information Photonics and Optical Communications, Beijing University of Posts and Telecommunications, Beijing 100876, China*
**Corresponding author: zhangwb@bupt.edu.cn; **corresponding author: xgzhang@bupt.edu.cn*
Received July 22, 2015; accepted November 26, 2015; posted online January 19, 2016

A new two-stage carrier-phase recovery scheme using a combination of an optical pilot-aided algorithm with the crossed constellation transformation algorithm for either square-framed or non-square-framed M-level-quadrature amplitude modulation (QAM) Nyquist systems is proposed. It is verified in 32- and 128-QAM systems that it can provide high linewidth tolerance with little complexity.

OCIS codes: 060.0060, 060.1660, 060.2330.
doi: 10.3788/COL201614.020601.

To meet the ever-increasing demands of high-speed, long-haul optical fiber communication systems, high-order modulation formats and superchannel signaling are two issues people are pursuing to achieve higher spectral efficiency. Compared to quadrature phase-shift keying, which has been adopted in the current commercial 100G coherent optical fiber communication system, M-level-quadrature amplitude modulation (M-QAM), in which M is more than 16, is the best candidate for next-generation 400G or 1T systems. Nyquist signaling and optical orthogonal frequency-domain multiplexing might also be used in 400G or 1T systems. In the former, a combination with M-QAM is preferred, because a Nyquist-M-QAM-wavelength-division multiplexing (WDM) system is more backward compatible with the current WDM system. Carrier-phase recovery (CPR) is a significant and integral part of the digital signal processing (DSP) procedure to compensate for the phase noise (PN) induced by both the transmitter and the local oscillator (LO) lasers. Many blind CPR algorithms have been proposed and demonstrated to mitigate the PN[1–10]. Among these methods, blind phase search (BPS) has the best linewidth tolerance for arbitrary M-QAM formats, but at the cost of high computation complexity[1]. Moreover, the algorithm's complexity increases as the QAM order (M) increases[11]. Many modified CPR algorithms have been introduced, such as maximum likelihood (ML) and constellation transformation (CT), to reduce the computation complexity, but with reduced linewidth tolerance[4,10].

In this work, a two-stage CPR scheme is proposed, in which the optical pilot-aided (PA) algorithm[7] works as the first stage and a so-called crossed constellation transformation (CCT) algorithm works as the second algorithm. Using the optical pilots just alongside the Nyquist-WDM signal bands, we can mitigate or compensate for impairments such as frequency offset, carrier PN, etc. because the pilots experience the same impairments from which the signals suffer. The analyses show that the proposed two-stage CPR scheme possesses a good linewidth tolerance for arbitrary M-QAM formats with much lesser complexity. Numerical simulations for dual-carriers Nyquist 32-QAM and 128-QAM optical communication systems using the proposed and other CPR methods are implemented. The performance of the PA + CCT CPR method is studied and compared with other CPR methods, such as only PA, PA + ML, and BPS.

Figure 1(a) shows the configuration of proposed optical PA dual-carriers Nyquist system. The laser light works at the frequency f_0, which is emitted by an external cavity

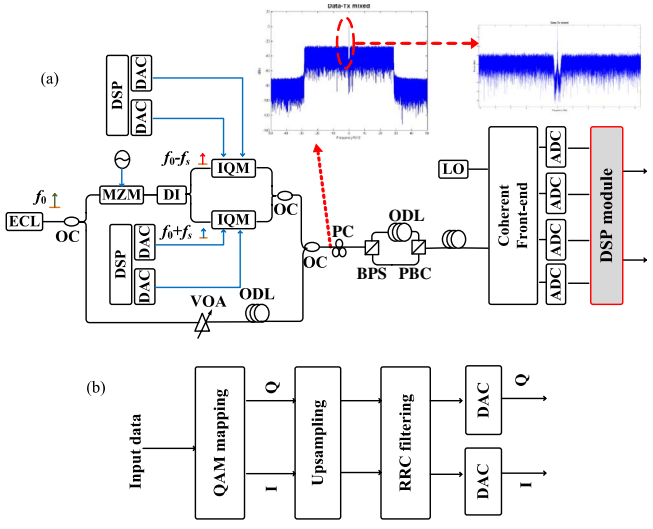

Fig. 1. (a) Proposed PA dual-carriers Nyquist transmission system. (b) Electrical Nyquist signal generation.

laser (ECL) split into two beams. One is used as pilot tone, while the other is modulated with the data through a Mach–Zenhder modulator driven by a sinusoidal RF signal with frequency $f_s = 14.5$ GHz to generate optical dual-carriers whose frequencies are $f_0 + f_s$ and $f_0 - f_s$:

$$\begin{aligned} E_{\text{out}}(t) &= A_{\text{in}} \cos(2\pi f_0 t) \sin[\gamma \sin(2\pi f_s t)] \\ &= A_{\text{in}} \cos(2\pi f_0 t)[2J_1(\gamma)\sin(2\pi f_s t) \\ &\quad + 2J_3(\gamma)\sin(2\pi f_s t) + \ldots] \\ &= A_{\text{in}}\{J_1(\gamma)\sin[2\pi(f_0 + f_s)t] \\ &\quad - J_1(\gamma)\sin[2\pi(f_0 - f_s)t + \text{hight order terms}\}. \end{aligned} \tag{1}$$

The two generated subcarriers are then separated by a delay interferometer (DI). Each subcarrier is modulated with a Nyquist M-QAM (e.g., 32- or 128-QAM) signal at the symbol rate of 28 Gbaud, which will lead to a pilot gap width of 1 GHz between two sub-channels and will sacrifice only 1.8% bandwidth overhead. A variable optical attenuator is used to adjust the pilot-to-signal ratio (PSR), and an optical delay line (ODL) is used to ensure phase synchronization between the pilot tone and two carrier signals. The Nyquist signal is then polarization multiplexed through a 50/50 splitter (BPS), an ODL, and a polarization beam combiner (PBC). At the receiver end, a coherent front end with an LO laser provides the electric signals corresponding to the I and Q components. After analog-to-digital conversion (ADC), these signals are processed by the DSP unit. In the simulation, we mainly focus on the laser phase estimation and carrier-phase recovery techniques in the Nyquist 32- or 128-QAM system, and assume that all the other impairments, such as chromatic dispersion and polarization mode dispersion, etc., are compensated for by the work in Refs. [12–14]. In the CPR process, the PA-CPR acts as the first stage to compensate for the PN, and the CCT algorithm following the PA-CPR acts as the second stage.

At the transmitter (Tx) end, the DSP block diagram for generating the Nyquist electrical 32-/128-QAM signal is shown in Fig. 1(b). The transmitted symbols are first mapped to a 32-/128-QAM constellation with I and Q tributaries. After being up-sampled to 2 samples/symbol, the 32-/128-QAM signal is fed into a 32-tap digital Nyquist root-raised cosine pulse shape filter with a 0.02 roll-off factor. Finally, digital-to-analog conversions (DAC) are carried out.

The basic principle of the proposed PA-CPR is to insert a pilot tone in the middle of the two sub-channels at the Tx end. As the pilot tone and the data signal are generated from same source and are exactly aligned in the time domain, they will experience the same PN caused by both the Tx and Rx lasers. Thus, we can use the information extracted from the pilot tone to compensate for the PN jointly in the both the sub-channels at the receiver end. The transmitted signal can be expressed as

$$\begin{aligned} E_{\text{Tx}}(t) &= \sqrt{E_s} M_1(t) e^{j[2\pi(f_0 - f_s)t + \theta_{\text{Tx}}(t)]} \\ &\quad + \sqrt{E_s} M_2(t) e^{j[2\pi(f_0 + f_s)t + \theta_{\text{Tx}}(t)]} \\ &\quad + \sqrt{E_{\text{pilot}}} e^{j[2\pi f_0 t + \theta_{\text{Tx}}(t)]}, \end{aligned} \tag{2}$$

where $M_1(t)$ and $M_2(t)$ are the signals of the two Nyquist data sub-channels modulated with 32- or 128-QAM, θ_{TX} is the PN caused by the Tx laser, and $\sqrt{E_s}$ and $\sqrt{E_{\text{pilot}}}$ are the amplitudes of the data signal and the pilot tone, respectively.

Through transmission in the optical fiber channel, for simplicity, only amplified spontaneous emission (ASE) noise induced by the erbium-doped fiber amplifiers is considered. The central frequency of the LO is f_0. If we consider the Rx laser to have a PN of θ_{RX}, the received signal can be written as

$$\begin{aligned} E_{\text{Rx}}(t) = \mu\Big(& \sqrt{E_s} M_1(t) e^{j[2\pi(-f_s)t + \theta_{\text{Tx}}(t) + \theta_{\text{Rx}}(t)]} \\ & + \sqrt{E_s} M_2(t) e^{j[2\pi f_s t + \theta_{\text{Tx}}(t) + \theta_{\text{Rx}}(t)]} \\ & + \sqrt{E_{\text{pilot}}} e^{j[\theta_{\text{Tx}}(t) + \theta_{\text{Rx}}(t)]} \Big) + n(t). \end{aligned} \tag{3}$$

Figure 2 shows the details of the implementation of the proposed two-stage carrier phase estimation scheme in the receiver's DSP module. In the first stage, PA-CPE is used. Two sub-channels and pilot tones are separated by using a digital frequency shifter and a low-pass filter (LPF) with a suitable order and bandwidth. After the pilot tone is filtered by the LPF, the instantaneous phase of the extracted pilot tone can be written as follows:

$$\theta_{\text{pilot}}(t) = \theta_{\text{Tx}}(t) + \theta_{\text{Rx}}(t) + \theta_n(t). \tag{4}$$

We can now easily extract the phase $\theta_{\text{pilot}}(t)$ as an estimated value for the compensation for the combined laser PN $\theta(t)$ induced by the Tx and Rx lasers, where the estimation error depends on $\theta_n(t)$.

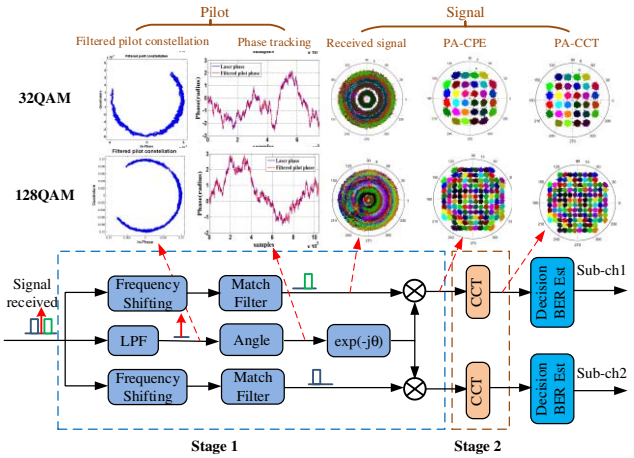

Fig. 2. DSP implementation of the multi-stage carrier-phase estimation scheme. The evolutions of the 32-QAM and 128-QAM constellations are shown in two stages.

In order to compensate for the residual phase shift, we employ the CCT phase estimation as the second stage of our proposed two-stage CPR algorithm. The key idea of the CCT algorithm is to transform the complex constellations down to the crossed-signal constellation, just like the transformations from Fig. 3(b) to 3(c). After the original constellations are transformed down to the crossed-signal constellation, we can easily use the conventional fourth-power method for the rest of the phase estimation. In addition, the CCT algorithm is not only suitable for square-frame QAMs like 16-QAM and 64-QAM, but also for non-square-frame QAMs like 32-QAM and 128-QAM, and hence it is more suitable to be the second stage after the PA-CPR algorithm because the PA-CPR is also modulation- format transparent. The transformation equation of the CCT is as follows:

$$C = I - A_I \,\mathrm{sign}[I - B_I \,\mathrm{sign}(I)] + i\{Q - A_Q \,\mathrm{sign}[Q - B_Q \,\mathrm{sign}(Q)]\}, \quad (5)$$

where I and Q are the real and imaginary parts of the coordinates, A_I and A_Q are the absolute values of the displacement components between the old points and the new points in the real and imaginary parts, B_I and B_Q are the absolute values of the coordinate points at the target location, and sign(·) is the sign function. The values of A_I, A_Q, B_I, and B_Q are different, and rely on the modulation formats. Figure 3 shows the transformation procedure of a 32-QAM (Figs. 3(b) and 3(c)) and a 128-QAM (Fig. 3(a)–3(c)) into the crossed constellation.

The simulation platform of a Nyquist 32-QAM or 128-QAM transmission system was constructed to investigate the performance of the proposed PA-CCT-CPR scheme. A total number of 2^{17} symbols at the symbol rate of 28 Gbaud was used in this simulation. The PN is modeled as a Wiener process with a variance of $\sigma^2 = 2\pi\Delta f \cdot T_s$, where Δf denotes the combined linewidth of the transmitter and the local lasers, and T_s is the symbol period. Different amounts of ASE noise are loaded to obtain different values of the optical signal-to noise ratio (OSNR), which is defined as the ratio of the optical power of the signal to the noise power with a 0.1 nm reference BW.

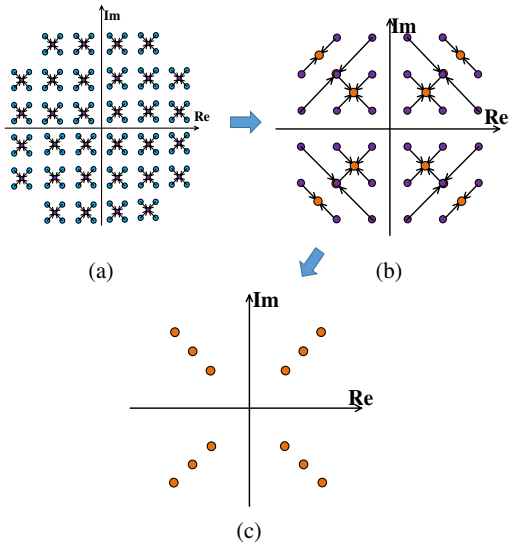

Fig. 3. Transformation procedures of 128-QAM and 32-QAM into the crossed-signal constellation.

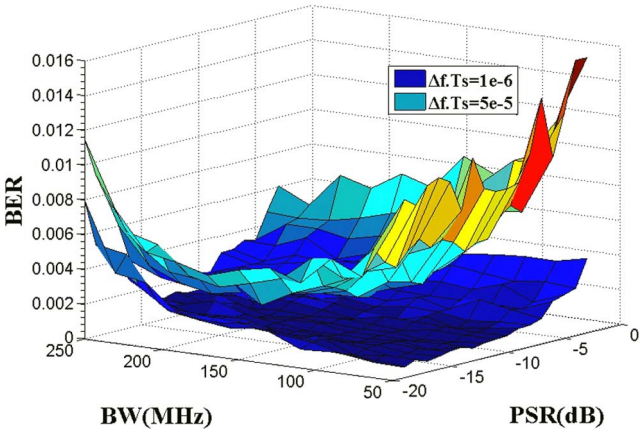

Fig. 4. BER surface versus PSR and the bandwidth of the pilot LPF at two different laser linewidths for 32-QAM.

There are two important parameters that have great influence on the performance of the PA-CPR. One is the PSR and the other is the bandwidth of the pilot-extracted LPF, which is denoted by B_{LPF}. In order to investigate the performance of the CPR scheme under

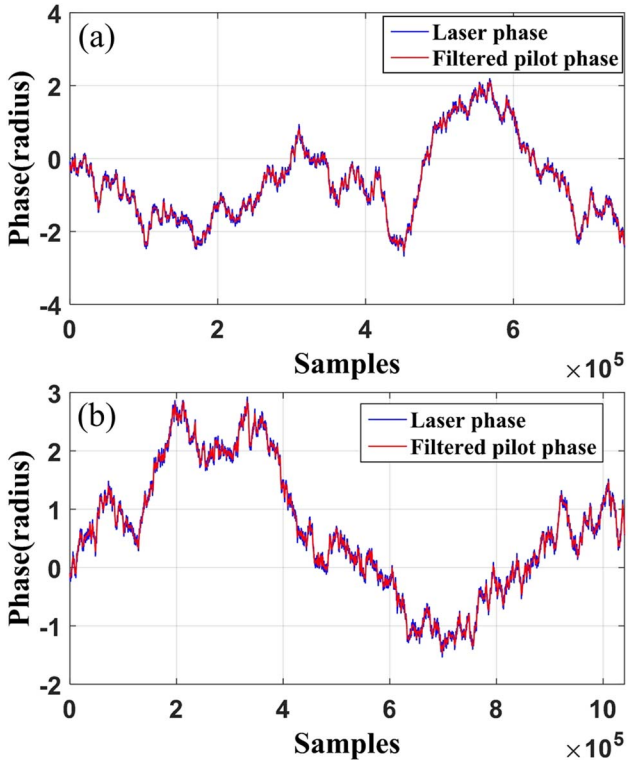

Fig. 5. Actual and estimated PN fluctuations by PA: (a) 32-QAM, and (b) 128-QAM.

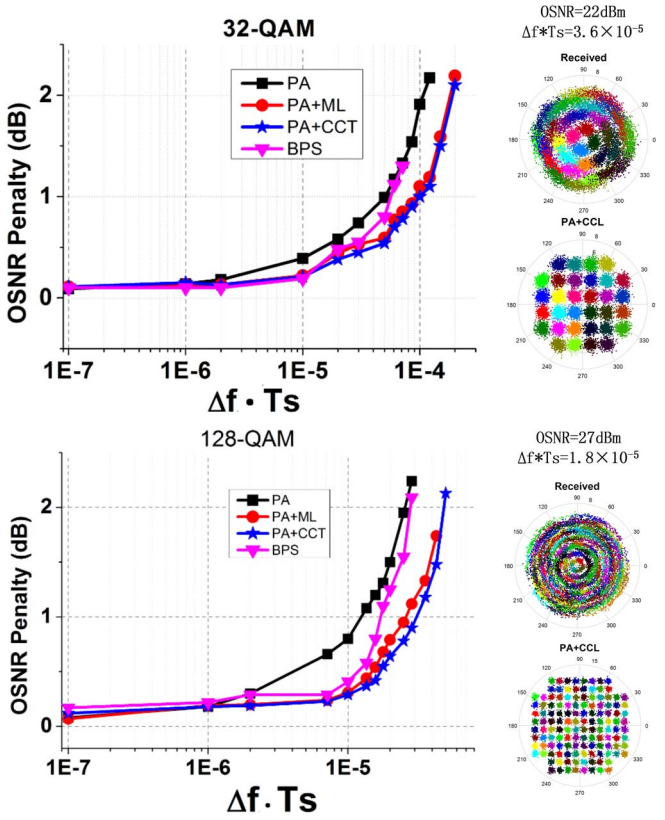

Fig. 6. (a) OSNR penalty versus linewidth symbol rate at BER $= 3.8 \times 10^{-3}$ for 32-QAM. (b) OSNR penalty versus linewidth symbol rate at BER $= 3.8 \times 10^{-3}$ for 128-QAM.

the different linewidths, the PSR and the B_{LPF} must be optimized simultaneously. We set the PSR to range from 20 to 3 dB and the B_{LPF} to range from 50 to 250 MHz. Figure 4 illustrates how the values of the PSR and B_{LPF} affect the performance of the 32-QAM system, where the lower and upper surfaces correspond to $\Delta f \cdot T_s = 1 \times 10^{-6}$ and $\Delta f \cdot T_s = 5 \times 10^{-5}$, respectively. It shows that as $\Delta f \cdot T_s$ increases, the optimum values of the PSR and B_{LPF} also increase. The optimal PSR and B_{BPF} values can be found based on the minimum value of the bit error rate (BER) under the different values of $\Delta f \cdot T_s$. In Fig. 4, the optimal combinations of the PSR and B_{BPF} (14 dB, 70 MHz) and (11 dB, 230 MHz) are found for $\Delta f \cdot T_s = 1 \times 10^{-6}$ and $\Delta f \cdot T_s = 5 \times 10^{-5}$, respectively. In the following calculations, the optimum values of the PSR and B_{LPF} are always considered for different $\Delta f \cdot T_s$.

In order to assess the performance of our proposed two-stage CPR algorithm in the Nyquist 32/128-QAM system, we first compare the actual PN induced jointly by the Tx and Rx lasers with the phase estimated by the extracted pilot, as shown in Fig. 5. The $\Delta f \cdot T_s$ is set to be 5×10^{-5}, and the OSNR is 23 dB in the Nyquist 32-QAM system and 30 dB in the Nyquist 128-QAM system. The figure confirms that the PA-CPR can correctly track the phase fluctuations caused by the laser PN under the different modulation formats. After compensating for the PN with the PA algorithm, a second-stage CCT method is implemented as the fine PN compensation to cope with the residual PN.

The performance of the PA + CCT CPR is assessed and compared to other CPR schemes in terms of the evaluation of linewidth tolerance for 32- and 128-QAM formats. Both the OSNR and linewidth are swept to get the curves of the OSNR penalty versus $\Delta f \cdot T_s$ at a BER of 3.8×10^{-3}. When the equivalent linewidth is 0 Hz, the OSNR required at a BER of 3.8×10^{-3} is regarded as the reference for the initial penalty. Figures 6(a) and 6(b) show the OSNR penalty as a function of $\Delta f \cdot T_s$ for 32-QAM and 128-QAM, respectively, and also give the color constellation diagrams of each QAM format on the right. The CPR schemes used in the comparison are PA only, PA + ML, PA + CCT, and BPS. We can find that all the CPR algorithms show low OSNR penalty requirements when the $\Delta f \cdot T_s$ takes small values. As the value of $\Delta f \cdot T_s$ increases, a larger OSNR is required. As shown in Fig. 6, for a large value of $\Delta f \cdot T_s$, it turns out that the two-stage PA + CCT CPR algorithm even shows a better performance than the BPS algorithm, which is known to have best linewidth tolerance, according to the literature. Moreover, the results show that PA + ML and PA + CCT have a similar linewidth tolerance for 32-QAM, while for 128-QAM, the performance of PA + CCT is a little better than that of the PA + ML.

Table 1 lists $(\Delta f \cdot T_s)_{\max}$ of the CPR schemes mentioned above and the corresponding tolerable linewidth values Δf for the 28 Gbaud Nyquist 32/128-QAM system. Here, we define the linewidth symbol rate $(\Delta f \cdot T_s)$ at a 1 dB OSNR penalty as the maximum tolerable linewidth value $(\Delta f \cdot T_s)_{\max}$. We can conclude that the proposed two-stage PA + CCT CPR scheme shows the best linewidth tolerance performance in the 32/128-QAM Nyquist system.

Table 1. Linewidth Tolerance of Various CPR Schemes for 32- and 128-QAM

	32-QAM		128-QAM	
CPR scheme	$(\Delta f \cdot T_s)_{\max}$	$\Delta f_{\max}$ at 28 Gbaud (MHz)	$(\Delta f \cdot T_s)_{\max}$	$\Delta f_{\max}$ at 28 Gbaud (kHz)
PA	0.5×10^{-4}	1.4	1.4×10^{-5}	380
PA + ML	0.9×10^{-4}	2.5	2.6×10^{-5}	740
PA + CCT	0.9×10^{-4}	2.5	2.9×10^{-5}	800
BPS	0.6×10^{-4}	1.7	1.8×10^{-5}	500

In comparison with the BPS method, the first-stage PA-CPR only needs to separate the pilot from the carrier signals with a BPF and extract the instantaneous phase to compensate for the PN directly. The BPF can be achieved by a digital finite impulse response filter, which is easy to implement in the hardware. Therefore, the proposed PA-CPR scheme has fewer operations and is less complex. The computation complexities of BPS, ML, and CT have been discussed in Ref. [3], and the conclusion is that the complexity of the CT algorithm is similar to that of the ML algorithm, but much lower than that of the BPS algorithm. In the present work, the mentioned CCT algorithm is another form of the CT algorithm. The difference is that CCT is suitable for non-squared-frame QAMs, and CT is not. Therefore, they have similar computation complexity. In conclusion, the proposed PA-CCT CPR has the best performance of linewidth tolerance, and is less complex than the BPS.

We propose an optical domain PA CPR scheme by insetting the optical pilot between two subcarriers, which can realize phase recoveries of both two-sided subcarriers at the same time and reduced the bandwidth overhead. The PSR and the bandwidth of the LPF are optimized. Using the optimal parameters, the performances of different CPR schemes are compared. PA+CCT shows good linewidth tolerance of $\Delta f \cdot T_s = 9 \times 10^{-5}$ (for 32-QAM) and $\Delta f \cdot T_s = 2.9 \times 10^{-5}$ (for 128-QAM) at a 1 dB OSNR penalty, which is better than the BPS and is much less complex.

This work was partly supported by the National Natural Science Foundation of China (Nos. 61205065 and 61571057), the Open Fund of IPOC (BUPT) (No. IPOC2013B005), the Fund of the State Key Laboratory of Information Photonics and Optical Communications (Beijing University of Posts and Telecommunications), and the Fundamental Research Funds for the Central Universities (No. 2014RC1201).

References

1. T. Pfau, S. Hoffmann, and R. Noé, J. Lightwave. Technol. **27**, 989 (2009).
2. X. Zhou, IEEE Photon. Technol. Lett. **22**, 1051 (2010).
3. J. H. Ke, K. P. Zhong, Y. Gao, J. C. Cartledge, A. Karar, S. Abdullah, and M. A. Mohammad, J. Lightwave Technol. **30**, 3987 (2012).
4. K. P. Zhong, J. H. Ke, Y. Gao, and J. C. Cartledge, J. Lightwave Technol. **31**, 50 (2013).
5. S. M. Bilal, C. R. S. Fludger, V. Curri, and G. Bosco, J. Lightwave Technol. **32**, 2973 (2014).
6. M. Morsy-Osman, Q. Zhuge, L. R. Chen, and D. V. Plant, Opt. Express **19**, 24331 (2011).
7. Z. Zhang, J. Lin, X. Su, L. Xi, Y. Qiao, and X. Zhang, Opt. Eng. **53**, 066108 (2014).
8. M. Morsy-Osman, Q. Zhuge, M. Chagnon, X. Xu, and D. V. Plant, in *Proceedings of OFC 2013* OTu31.6 (2013).
9. K. Kikuchi, in *Proceedings of ECOC 2008* Th.2.A.1 (2008).
10. Y. Gao, A. P. T. Lau, S. Y. Yan, and C. Lu, Opt. Express **19**, 21717 (2011).
11. S. M. Bilal, G. Bosco, P. Poggiolini, and C. R. S. Fludger, in *Proceedings of ECOC 2013* 966 (2013).
12. W. Huang, D. Liu, X. Zhang, and Y. Zhang, Chin. Opt. Lett. **9**, 080101 (2011).
13. Y. Sun, L. Xi, X. Tang, D. Zhao, Y. Qiao, X. Zhang, and X. G. Zhang, Chin. Opt. Lett. **12**, 100606 (2014).
14. J. Zhang, Y. Gu, X. Yuan, F. Tian, X. Zhang, and J. Tao, Chin. Opt. Lett. **10**, 030607 (2012).